Available online at www.sciencedirect.com
ScienceDirect
International Journal of Mass Spectrometry 267 (2007) 277–283
www.elsevier.com/locate/ijms

Dissociation of chloride from *ortho*-, *meta*- and *para*-chloromethylphenoxides: The enthalpy of formation of *meta*-quinomethane

Silvi A. Chacko, Paul G. Wenthold *

The Department of Chemistry, Purdue University, West Lafayette, IN 47906-2084, United States

Received 1 November 2006; received in revised form 23 February 2007; accepted 27 February 2007
Available online 4 March 2007

Dedicated to the memory of Sharon Lias, in recognition of all her contributions to the field of ion thermochemistry.

Abstract

The enthalpy of formation of *m*-quinomethane has been determined by energy-resolved collision-induced dissociation measurements involving chloro-substituted phenoxide ions. The chloride affinity of *m*-quinomethane is measured to be 202 ± 9 kJ/mol, whereas the chloride affinities of *o*- and *p*-quinomethane are both 57 ± 5 kJ/mol. The difference in the chloride affinities reflects the difference in the stabilities of the Kekule and non-Kekule structures. Combination of the dissociation energy of the *meta*-isomer with the gas-phase acidity of 3-(chloromethyl)phenol, measured by using the kinetic method to be 1432 ± 6 kJ/mol, results in an enthalpy of formation of 166 ± 13 kJ/mol for the *m*-quinomethane diradical. The measured value agrees with that predicted by bond additivity. The low bond dissociation energies for the *o*- and *p*-isomers, along with electronic structure calculations, suggest that the corresponding chlorine-substituted ions are best described as halide/diradical complexes.

Keywords: Quinomethane; Non-Kekule structure; Halide/diradical complex

1. Introduction

Quinones (**1**), quinomethanes (**2**) and quinodimethanes (**3**) are substituted aromatic molecules that differ by the presence of oxygen atoms or methylene groups [1].

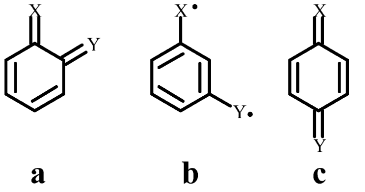

1: X = Y = O
2: X = O, Y = CH$_2$
3: X = Y = CH$_2$

These didehydro-substrates, which result from homolytic cleavage of aromatic O–H and C–H bonds in hydroquinones, cresols and xylenes, respectively, are interesting for both practical and fundamental reasons. For example, quinones occur widely in nature and are found in a variety of pigments and medicines [2,3]. They play significant roles in photochemical processes, oxidation–reduction reactions, photosynthesis and are precursors for synthetic transformations [4,5]. In addition, alkylated quinones, such as **2c**, have been discovered to play important roles in biochemical processes, such as protein and DNA alkylation [6], and quinomethanes, **2**, are critical reactive intermediates formed in the biotransformation of lignin and certain anticancer or antibiotic drugs [7–11]. As benzylic precursors [12], quinomethanes are extremely useful in organic synthesis because they can be exploited for carbon–carbon bond formation or in reactions with nucleophiles [7,13–16]. Due to their ability to act as Michael acceptors [6] they can cause harmful effects in vivo, including immunotoxicity, cytotoxicity and carcinogenesis [17,18]. For example, butylated hydroxytoluene undergoes oxidation by an isoform of Cyt P450 in the lung cells, and the hydroxylated structure can be modified into a reactive intermediate that can undergo covalent binding, leading to cytotoxicity [19].

---

* Corresponding author. Tel.: +1 765 494 0475; fax: +1 765 494 0239.
E-mail address: pgw@purdue.edu (P.G. Wenthold).

1387-3806/$ – see front matter © 2007 Elsevier B.V. All rights reserved.
doi:10.1016/j.ijms.2007.02.052

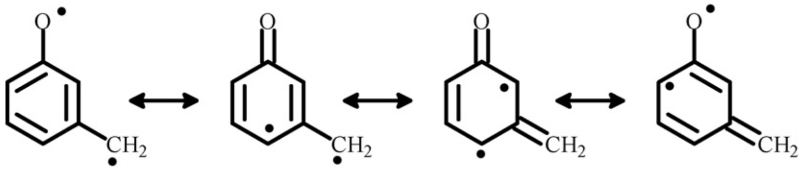

Scheme 1.

The *ortho*- and *para*-isomers of quinomethane (**2a**, **2c**) are examples of Kekule structures, where resonance forms can be drawn in which all the electrons can be paired. Conversely, *m*-quinomethane (**2b**) is a non-Kekule structure, because it is not possible to draw a resonance structure in which all the electrons are paired (Scheme 1). *o*-Quinomethane, **2a**, its substituted analogues, and *p*-quinomethane, **2c**, have closed-shell electronic structures and are well known in condensed-phase synthetic chemistry [7,20–28]. Similarly, **2b** has been characterized by UV–vis optical absorption spectroscopy [29] and electron paramagnetic resonance (EPR) spectroscopy [30,31]. In addition, **2b** undergoes cycloaddition reaction with dienes, presumably through a zwitterionic, monocyclic, singlet reactive intermediate [32]. The *meta*-diradical can be generated by photochemical or thermal ring cleavage of 6-methylenebicyclo[3.1.0]hex-3-en-2-one [29].

Simple methods have been developed in order to predict the electronic ground states of molecules like **1–3** [33–37]. In all cases, the ground states for the Kekule isomers are predicted to be singlets, whereas those for the non-Kekule, *meta*-isomers are predicted to be triplets. The singlet ground states of the *ortho*- [25] and *para*-isomers [28] are well established for **1–3** [1]. Triplet ground states have been confirmed for **1b** and **3b**, and the spectroscopic data and reactivity of **2b** are consistent with the presence of a triplet ground state, as well [29,32].

The differences in the electronic properties of the ground states of the *ortho*-, *meta*- and *para*-isomers are reflected in their thermochemical stabilities. Enthalpies of formation for many of the species have been measured by using mass spectrometric methods. For example, Hehre and co-workers [38] determined the enthalpies of formation of **3a** and **3c** by bracketing the energy for proton transfer from the methyl-substituted benzyl cations (Eqs. (1a) and (1b)) [38]. By using the bracketed proton affinity values along with the enthalpies of formation of the benzyl cations, the heats of formation of **3a** and **3c** were determined to be 209 and 222 kJ/mol, respectively [38]. The measured energies for **3a** and **3c** are more than 100 kJ/mol lower than that for *m*-xylylene, **3b**, which was determined by Hammad and Wenthold [39] by using a combination of ion proton affinity and energy-resolved CID measurements. Similarly, Kass and co-workers [40] measured the energy of formation of *m*-quinone, **1b**, and found it to be 28.5 kJ/mol, whereas the enthalpies of formation for the *ortho*- and *para*-isomers are −96.7 and −115.9 kJ/mol [16].

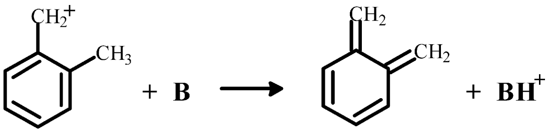

3a

(1a)

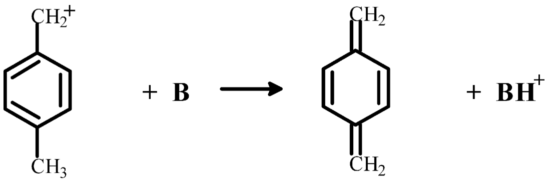

3c

(1b)

The thermochemical properties of quinomethanes, **2**, have not been investigated to the same extent as have those for **1** and **3**. Previously reported studies [41] have determined the proton affinities of **2a** and **2c** (Eqs. (2a) and (2b)), but they cannot be used to determine the enthalpies of formation of the reactive species because the energies of the corresponding benzyl cations are not known. In this work, we report an investigation of the isomeric quinomethanes, **2a–c**, by using energy-resolved collision-induced dissociation (CID) [42,43] of the *o*-, *m*- and *p*-chloromethylphenoxide ions, **4a–c**, as shown in Scheme 2.

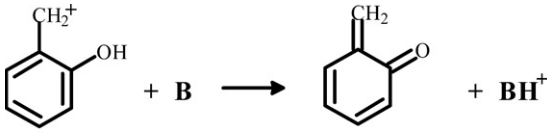

2a

(2a)

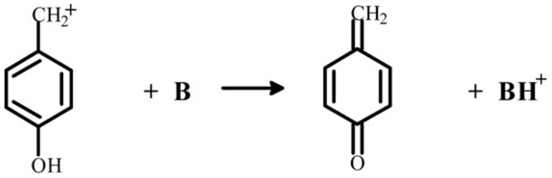

2c

(2b)

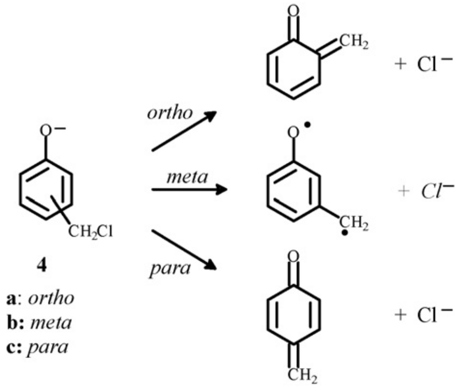

Scheme 2.

The enthalpy of formation of *m*-quinomethane (**2b**) has been measured by combining the energy for halide loss with the gas-phase acidity of 3-chloromethylphenol. The dissociation energies of the 2- and 4-chloromethylphenoxide ions are much lower than that for the *meta*-isomer, consistent with the formation of highly stable products. Electronic structure calculations indicate significant lengthening of the C–Cl bond lengths in the ions of the *ortho*- and *para*-substituted phenoxide ions, suggesting that the ions might be better described as "halide–biradical complexes" [44].

2. Experimental

All experiments were carried out in a flowing afterglow-triple quadrupole instrument that has been described elsewhere [45,46]. The primary reactant ion, F^- was prepared by 70 eV electron ionization of fluorine gas (5% in He). The ions are carried by helium buffer gas (0.400 Torr, flow (He) = 190 STP cm^3/s) through the flow tube (1 m × 7.3 cm) where they are allowed to react with neutral reagent vapors, added through micrometering or leak valves. The ions in the flow tube undergo $\sim 10^5$ collisions with the helium buffer gas before being extracted from the flow tube through a 1 mm sampling orifice, where they are focused into a triple quadrupole analyzer.

Energy-resolved mass spectrometry experiments are carried out by selecting ions with the desired mass-to-charge ratio by using the first quadrupole and injecting them into the second quadrupole (q2, radio frequency only) where they undergo collision-induced dissociation with argon or neon target, using neon for reactions with very low dissociation energies. Product ions are mass analyzed with the third quadrupole and detected with a channeltron electron multiplier operated in pulse counting mode. The collision energy of the primary ion in q2 was varied and fragment ion intensities were monitored as a function of q2 rod offset voltage to yield energy-resolved mass spectra, with the energy zero determined by using retarding potential analysis.

Cross-sections for CID, σ, were calculated using $I/I_o = \sigma Nl$, where I and I_o are the intensities of the product and reactant ions, respectively, N the number density of the target and l is the effective collision path length. The effective path length was measured to be 24 ± 4 cm [46] by using the reaction of $Ar^+ + D_2 \rightarrow ArD^+ + D$ [47]. Cross-sections are measured at several different pressures ranging from 0.075 to 0.200 mTorr, and extrapolated to zero pressure, corresponding to single collision conditions.

2.1. Data analysis

Energy-resolved cross-sections were modeled with the expression shown in Eq. (3) [48,49], where E is the center-of-mass collision energy of the reactant ion, g_i the fraction of the ions with internal energy E_i, E_0 the threshold energy for dissociation, n the parameter that reflects the energy deposition in the collision [50] and σ_0 is a scaling factor. Also convoluted into the fit were the ion kinetic energy distributions, approximated as a Gaussian function with a 1.5 eV (laboratory frame) full-width at half-maximum, and a Doppler broadening function to account for motion of the target gas. The factor P_i is the probability for ion dissociation, calculated from RRKM theory. A loose, orbiting transition state was assumed for the process, corresponding to the phase space limit [51,52], with the constants calculated by using the calculated properties of the products.

$$\sigma(E) = \sigma_0 \sum_i \frac{P_i g_i (E + E_i - E_0)^n}{E} \tag{3}$$

The data are modeled by adjusting the parameters to correspond with the steeply rising portion of the appearance curve directly above the onset. Data analysis and modeling of the cross-sections were carried out using the CRUNCH 5 program developed by Armentrout and co-workers [47–49,51,52]. Modeled threshold energies, E_0, are 0 K ΔE values and were converted to 298 K bond dissociation enthalpies by using the integrated heat capacities of reactants and products, obtained from electronic structure calculations. Uncertainties in enthalpy values were calculated by statistical combination of the standard deviation of values obtained from replicate experimental trials, the uncertainty in the absolute energy scale for the experiment (estimated to be 0.15 eV laboratory frame), and a contribution due to uncertainty in the transition state model. The uncertainty in the transition state was estimated as the change in dissociation energy when raising and lowering the frequencies of the transition state so to cause a 8 J/(mol K) change in the activation entropy for the reaction. A contribution is also included to account for uncertainty in the chosen fitting range of the data, which is estimated by finding the effect on the data.

2.2. Computational methods

Geometries, absolute energies, vibrational frequencies and enthalpies for isomers of chloromethyl phenoxides were calculated using density functional theory (B3LYP), using Gaussian 03 [53].

2.3. Materials

The 3-(chloromethyl)phenol was prepared by demethylation of the commercially available methyl ether by reaction with 1.0 M BBr_3 [54]. The 2-(chloromethyl)phenyl and 4-(chloromethyl)phenyl acetates were obtained from commercial sources and used as supplied. Liquid samples were degassed by successive freeze–pump–thaw cycles prior to use. Helium was purified via a liquid nitrogen trap containing molecular sieves. Gas purities are as follows: He (99.995%), F_2 (5% in helium), Ar (99%), Ne (99%).

3. Results

In this section, we describe the measurements of the dissociation energies for loss of chloride from *o*-, *m*- and *p*-chloromethylphenoxide ions, and the determination of the enthalpy of formation of *m*-quinomethane.

3.1. Ion generation

The *o*- and *p*-chloromethyl phenoxide ions were generated by chemical ionization of the corresponding acetates by F^-. The phenoxide ions are presumably formed by an addition/elimination reaction at the carbonyl, as shown for the *ortho*-isomer in Eq. (4), or an E2 elimination to form ketene and HF. Both reactions are estimated to be highly exothermic [55]. The addition/elimination reaction is more exothermic than E2 elimination ($\Delta H \approx -150$ kJ/mol for the addition/elimination process and -60 kJ/mol for the E2 reaction), whereas the E2 reaction is entropically favored.

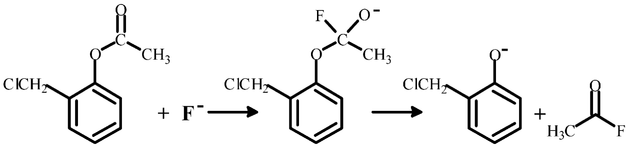

4a (4)

The 3-(chloromethyl)phenoxide ion was formed directly by deprotonation of 3-(chloromethyl)phenol using F^- as the base. Chloride anion is also observed as a product in the ionization, with an intensity that is ~5% of that of the phenoxide ions for the *meta*-isomer and ~15% for the *ortho*- and *para*-isomer.

3.2. CID of phenoxide ions

Chloride is the only product observed upon CID of the chloromethylphenoxide ions, **4a**–**c**. Energy-resolved cross-sections for the formation of chloride are shown in Fig. 1. Because the dissociation energies of **4a** and **4c** were very low, neon was used as the target for the CID of those ions. CID of **4b** was carried out using argon as the collision target. In the center-of-mass frame of reference, the threshold energies for formation of chloride **4a** and **4c** are essentially the same, and are much lower than that for **4b**, consistent with the expected relative stabilities of products **2a**–**c**. Modeling the data by using the procedures described in Section 2 gives the parameters listed in Table 1. In particular, the 298 K dissociation enthalpies are found to be 57 ± 5, 202 ± 9 and 57 ± 5 kJ/mol for **4a**, **4b** and **4c**, respectively.

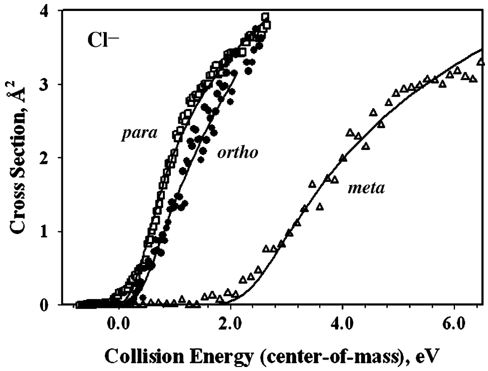

Fig. 1. Energy-resolved cross-sections for chloride formation from *o*-, *m*- and *p*-(chloromethyl)phenoxide ions, along with convoluted fits to the data. Argon was used as the CID target for the *meta*-ion, whereas neon target was used for the *ortho*- and *para*-isomers.

Table 1
Modeling parameters obtained from fits of CID cross-sections in Fig. 1

Chloromethyl phenoxide ion	ΔH_{298} (kJ/mol)	n	$\Delta S^{\ddagger}$ (J/(mol K))[a]
ortho-, **4a**	57 ± 5	1.5 ± 0.1	57
meta-, **4b**	202 ± 9	1.2 ± 0.1	48
para-, **4c**	57 ± 5	1.1 ± 0.1	48

‡ Standard notation for activation entropy.
[a] Activation entropy at 1000 K.

3.3. Acidity of 3-(chloromethyl)phenol

Although the dissociation energies reflect the general thermochemical properties of the products being generated, they also reflect the differences in the stabilities of the anions, as determined by the gas-phase acidities of the neutral phenols. The thermochemical relationship between dissociation energy ($\Delta H_{\mathrm{rxn}}(\mathrm{OC_6H_4CH_2{-}Cl^-})$), gas-phase acidity ($\Delta H_{\mathrm{acid}}$), and product enthalpy of formation is shown in Eq. (5). As such, Eq. (5) can be used to determine the enthalpy of formation of the quinomethanes, $\Delta H_{\mathrm{f,298}}(\mathrm{OC_6H_4CH_2})$, if the gas-phase acidity of the neutral precursor, $\mathrm{HOC_6H_4CH_2Cl}$, is known. In this work, we have measured the gas-phase acidity of 3-(chloromethyl)phenol, with which the enthalpy of formation of **2b** can be determined. Unfortunately, weak chloride binding in ions **4a** and **4c** make gas-phase acidities measurements for 2- and 4-(chloromethyl)phenol impractical.

$$\begin{aligned}&\Delta H_{\mathrm{f,298}}(\mathrm{OC_6H_4CH_2})\\&\quad= \Delta H_{\mathrm{rxn}}(\mathrm{OC_6H_4CH_2{-}Cl^-}) + \Delta H_{\mathrm{acid}}(\mathrm{HOC_6H_4CH_2Cl})\\&\qquad+ \Delta H_{\mathrm{f,298}}(\mathrm{HOC_6H_4CH_2Cl}) - \Delta H_{\mathrm{acid}}(\mathrm{HCl})\\&\qquad- \Delta H_{\mathrm{f,298}}(\mathrm{HCl})\end{aligned} \tag{5}$$

The gas-phase acidity of 3-(chloromethyl)phenol was determined by using the kinetic method, developed by Cooks and co-workers [56,57]. Proton-bound dimers of **4b** with a series of references, HB_i, were subjected to CID over an energy range of 3–5.5 eV (center-of-mass frame). At any given energy, the relationship between the measured branching ratio, $r_{\mathrm{E}} = I(\mathrm{B}_i^-)/I(\mathrm{RCl}^-)$, and the difference in the gas-phase acidities of 3-(chloromethyl)phenol, $\Delta H_{\mathrm{acid}}(\mathrm{HRCl})$, and the reference, $\Delta H_{\mathrm{acid}}(\mathrm{HB}_i)$, is given by Eq. (6), where $T_{\mathrm{eff,E}}$ is the effective temperature at the dissociation energy and $\Delta\Delta S$ is the difference in the activation entropies for the two dissociation channels.

$$\ln r_{\mathrm{E}} = \frac{\Delta H_{\mathrm{acid}}(\mathrm{HRCl}) - \Delta H_{\mathrm{acid}}(\mathrm{HB}_i) + \Delta\Delta S}{RT_{\mathrm{eff,E}}} \tag{6}$$

A plot of $\ln r_{\mathrm{E}}$ versus $\Delta H_{\mathrm{acid}}(\mathrm{B}_i)$ at energy E has a slope $m_{\mathrm{E}} = -1/RT_{\mathrm{eff,E}}$ and an intercept $y_{\mathrm{E}} = (\Delta H_{\mathrm{acid}}(\mathrm{HRCl})/RT) + (\Delta\Delta S/R)$. The gas-phase acidity of 3-(chloromethyl)phenol is obtained from a second regression plot of y_{E} versus $-m_{\mathrm{E}}$, which has a slope of $\Delta H(\mathrm{HRCl})$ and an intercept $\Delta\Delta S/R$. As noted by Armentrout [58], the slope and intercept of the first regression plot are strongly correlated. The correlation can be eliminated by plotting the $\ln r_E$ values versus $\Delta H_{acid}(B_i) - \Delta H_{acid}(avg)$, where $\Delta H_{acid}(avg)$ is the average gas-phase acidities of the reference acids. In this formulation, the slope of the second plot is $\Delta H_{acid}(HRCl) - \Delta H_{acid}(avg)$.

The measured branching ratios over the energy range considered are shown in Fig. 2a. The references used in this work include 3-fluorophenol ($\Delta H_{acid} = 1438 \pm 8.8$ kJ/mol), 4-fluorophenol ($\Delta H_{acid} = 1451 \pm 8.8$ kJ/mol), 3-chlorophenol ($\Delta H_{acid} = 1431 \pm 15$ kJ/mol) and 4-chlorophenol ($\Delta H_{acid} = 1436 \pm 8.8$ kJ/mol) [59]. The references were chosen because they have acidities similar to that expected for 3-(chloromethyl)phenol and because they do not have any substituents in the *ortho*-positions that would sterically affect the structure of the proton bound dimer, thereby minimizing the significance of $\Delta\Delta S$. Representative plots of $\ln r_E$ versus $\Delta H_{acid}(B_i) - \Delta H_{acid}(avg)$ at collision energies 3, 4 and 5 eV, are shown in Fig. 2b. The slopes of the lines imply effective temperatures of 580, 770 and 990 K at 3, 4 and 5 eV, respectively. The second regression plot, along with a linear fit to the data, is shown in Fig. 2c. The linear fit has a slope of -7 ± 4 kJ/mol, where the uncertainty includes the statistical error of the linear fit and an estimated 50% uncertainty in the measured effective temperature at each energy [60,61]. The average acidity of the references, $\Delta H_{acid}(avg)$, is 1439 ± 7, where the uncertainty assumes that half of the uncertainty in the reference acidities is an absolute uncertainty and half is random uncertainty. The measured slope, when combined with $\Delta H_{acid}(avg)$, gives a gas-phase acidity value of 1432 ± 8 kJ/mol. The intercept of the second regression plot is -1.7 ± 0.9 which corresponds to $\Delta\Delta S = 14 \pm 8$ J/(mol K). The relatively small value of $\Delta\Delta S$ reflects the structural similarity between the chloromethylphenol and the reference acids.

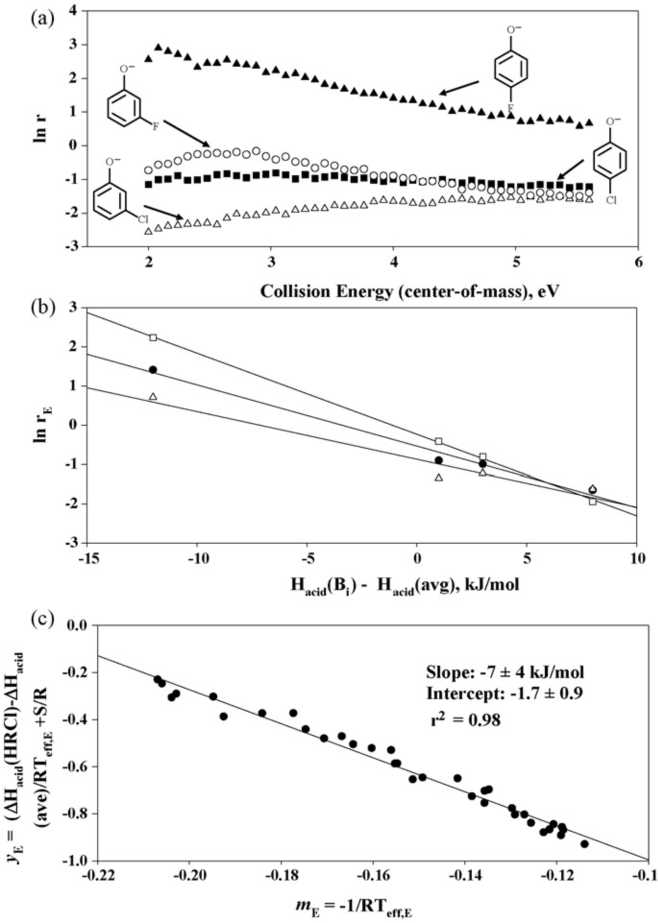

Fig. 2. Kinetic method plots for the determination of the acidity of 3-(chloromethylphenol). (a) Measured branching ratios as a function of energy; (b) representative plots of $\ln r$ vs. $\Delta H_{acid}(B_i) - \Delta H_{acid}(avg)$ at collision energies 3, 4 and 5 eV (center-of-mass frame of reference); (c) second regression plot to determine the gas-phase acidity.

3.4. Enthalpy of formation of m-quinomethane

The enthalpy of formation of **2b** can be calculated by using the relationship shown in Eq. (5). Although the enthalpy of formation of 3-(chloromethyl)phenol, $\Delta H_{f,298}(HOC_6H_4CH_2Cl)$, has not been measured previously, it can be reliably estimated by assuming that difference in the enthalpies of formation of 3-(chloromethyl)phenol and *m*-cresol is the same as that for benzylchloride and toluene. The assumption is supported at the B3LYP/6-31G* level of theory, as the enthalpy of the reaction shown in Eq. (7) is calculated to be 0.5 kJ/mol. Thus, the enthalpy of formation of 3-(chloromethyl)phenol is estimated to be -165 ± 4 kJ/mol. The enthalpy of formation of **2b**, calculated by using Eq. (5), is 166 ± 13 kJ/mol.

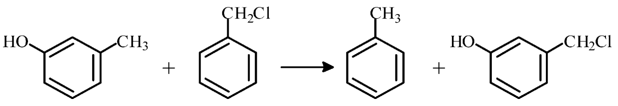

(7)

4. Discussion

4.1. Enthalpy of formation of **2b**

The relative dissociation energies of **4a–c** shown in Table 1 predominantly reflect the relative stabilities of neutral products **2a–c**. Formation of the more stable, closed-shell neutral products requires a much lower dissociation energy than formation of the triplet diradical. Previous studies of the π,π-*m*-phenylene diradicals **1b** [40] and **3b** [39] have found that their enthalpies of formation are generally consistent with the values predicted by bond additivity. The bond additivity estimation for the enthalpy formation of **2b** is illustrated in Eq. (8). Assuming that the O–H and α-C–H bonds in *m*-cresol have the same values as those in phenol (371 ± 3 kJ/mol) [62] and toluene (375.3 ± 2.5 kJ/mol) [63], respectively, the enthalpy of formation of **2b** is predicted to be 173 ± 6 kJ/mol, which agrees with the measured value of 166 ± 13 kJ/mol. The agreement between the measured enthalpy of formation of **2b** and the bond additivity estimate indicates that intersystem crossing is rapid during the nominally spin-forbidden reaction.

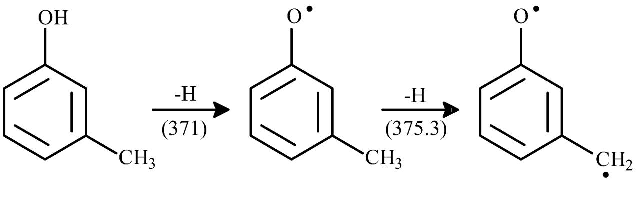

(8)

4.2. Structures of 2- and 4-(chloromethyl)phenoxide ions

The acidities of 2- and 4-(chloromethyl)phenol have not been measured in this work because the structures of the conjugate base anions are not necessarily well defined. Although they may have the chloromethyl-substituted phenoxide ion structure, as reflected in the structure of **4a**, the low-dissociation energies for loss of chloride are in the range of those weakly bound cluster ions [59,64]. Linnert and Riveros [44] have reported that ion–benzyne complexes can be formed by deprotonation of bromo- and iodobenzene.

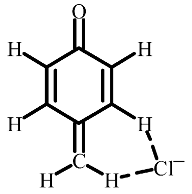

5c

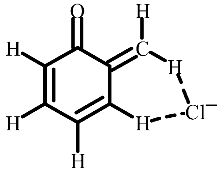

5a

Electronic structure calculations support the assessment of **4a** and **4c** as halide–diradical complexes. At the B3LYP/6-31 + G* level of theory, the ion–diradical complexes, **5a** and **5c**, are found to have 298 K enthalpies that are 1 kJ/mol higher and lower than the phenoxide structures, respectively. More importantly, the calculated 298 K free energies of **5a** and **5c** are ~3 kJ/mol lower than those of the phenoxide ions. The phenoxide ions themselves even exhibit properties that suggest a halide/diradical complex. For example, the C–Cl bonds in **4a** and **4c** are calculated to be 1.99 and 2.55 Å, significantly longer than the corresponding bond length in **4b**, 1.89 Å. Similarly, the Mullikin charge densities indicate that the negative charge in the ions is located on the chloride ions, and not on the phenoxyl oxygen. Therefore, it is not surprising that the ion prefers to adopt a structure where the ion has completely dissociated from the aromatic π system.

5. Conclusions

The enthalpy of formation of the *m*-quinomethane biradical has been determined by using a thermochemical cycle that combines acidity measurements and energy-resolved collision-induced dissociation. The measured enthalpy of formation, 166 ± 13 kJ/mol, agrees with the value predicted by bond additivity, as expected for the triplet diradical. The halide bond dissociation energies for the 2- and 4-(chloromethyl)phenoxide ions are much lower than that for the *meta*-isomer, consistent with the expected differences in stabilities of the neutral products. The low halide binding energies and computational studies suggest that the 2- and 4-(chloromethyl)phenoxide ions have unusually long C–Cl bonds, and may actually exist as halide–diradical complexes.

Acknowledgements

This work was supported by the National Science Foundation [CHE02-54874] and by the Petroleum Research Fund, administered by the American Chemical Society.

References

[1] P. Wan, D.W. Brousmiche, C.Z. Chen, J. Cole, M. Lukeman, M. Xu, Pure Appl. Chem. 73 (2001) 529.
[2] R.A. Morton, Biochemistry of Quinones, Academic Press, New York, 1965.
[3] R.H. Thompson, Naturally Occurring Quinones, second ed., Academic Press, New York, 1971.
[4] S. Patai, Z. Rappoport, The Chemistry of Quinonoid Compounds, Wiley, New York, 1974.
[5] S. Patai, Z. Rappoport, The Chemistry of Quinonoid Compounds, vol. 2, Wiley, New York, 1988.
[6] H.M. Awad, M.G. Boersma, S. Boeren, H.v.d. Woude, J.v. Zanden, P.J.v. Bladeren, J. Vervoort, I.M.C.M. Rietjens, FEBS Lett. 520 (2002) 30.
[7] P. Wan, B. Barker, L. Diao, M. Fischer, Y. Shi, C. Yang, Can. J. Chem. 74 (1996) 465.
[8] S.M. Shevchenko, A.G. Apushkinskii, Russ. Chem. Rev. 61 (1992) 1.
[9] D.C. Thompson, J.A. Thompson, M. Sugumaran, P. Moldeus, Chem. Biol. Interact. 86 (1992) 126.
[10] M.G. Peter, Angew. Chem. Int. Ed. Engl. 28 (1989) 555.
[11] P. Pande, J. Shearer, J. Yang, W.A. Greenberg, S.E. Rokita, J. Am. Chem. Soc. 121 (1999) 6773.
[12] M.A. Sanner, M. Stansberry, C. Weigelt, W.F. Michne, Tetrahedron Lett. 33 (1992) 5287.
[13] W. Baik, H.J. Lee, S. Koo, B.H. Kim, Tetrahedron Lett. 39 (1998) 8125.
[14] R.W.v.d. Water, T.R.R. Pettus, Tetrahedron 2002 (2002) 5367.
[15] M.P. Green, S. Pichlmair, M.M.B. Marques, H.J. Martin, O. Diwald, T. Berger, J. Mulzer, Org. Lett. 8 (2004) 3131.
[16] J.E. Ezcurra, K. Karabelas, H.W. Moore, Tetrahedron 61 (2005) 275.
[17] J.L. Bolton, E. Pisha, F. Zhang, S. Qiu, Chem. Res. Toxicol. 11 (1998) 1113.
[18] J.L. Bolton, M.A. Trush, P.T.M.G. Dryhurst, T.J. Monks, Chem. Res. Toxicol. 13 (2000) 135.
[19] T.F. Woolf, Handbook of Drug Metabolism, 1999, p. 265.
[20] L. Diao, C. Yang, P. Wan, J. Am. Chem. Soc. 117 (1995) 5369.
[21] R.A. McClelland, Tetrahedron 52 (1996) 6823.
[22] E. Modica, R. Zanaletti, M. Freccero, M. Mella, J. Org. Chem. 66 (2001) 41.
[23] B. Barker, L. Diao, P. Wan, Photochem. Photobiol. A 104 (1997) 91.
[24] T. Rosenau, A. Potthast, T. Elder, P. Kosma, Org. Lett. 4 (2002) 4285.
[25] Y. Chiang, A.J. Kresge, Y. Zhu, J. Am. Chem. Soc. 123 (2001) 8089.
[26] Y. Chiang, A.J. Kresge, Y. Zhu, J. Am. Chem. Soc. 124 (2002) 717.
[27] Y. Chiang, A.J. Kresge, Y. Zhu, Photochem. Photobiol. Sci. 1 (2002) 67.
[28] Y. Chiang, A.J. Kresge, Y. Zhu, J. Am. Chem. Soc. 2002 (2002) 6349.
[29] D.E. Seeger, P.M. Lahti, A.R. Rossi, J.A. Berson, J. Am. Chem. Soc. 108 (1986) 1251.
[30] M. Rule, A.R. Matlin, E.F. Hilinski, D.A. Dougherty, J.A. Berson, J. Am. Chem. Soc. 101 (1979) 5098.
[31] T.A. Inglin, J.A. Berson, J. Am. Chem. Soc. 108 (1986) 3394.
[32] A.R. Matlin, T.A. Inglin, J.A. Berson, J. Am. Chem. Soc. 104 (1982) 4954.
[33] W.T. Borden, Mol. Cryst. Liquid Cryst. Sci. Technol., Sect. A: Mol. Cryst. Liquid Cryst. 232 (1993) 195.
[34] H.C. Longuet-Higgins, J. Chem. Phys. 18 (1950) 283.
[35] W.T. Borden, E.R. Davidson, J. Am. Chem. Soc. 99 (1977) 4587.
[36] A.A. Ovchinnikov, Theor. Chem. Acta 47 (1978) 297.
[37] I.A. Misurkin, A.A. Ovchinnikov, Russ. Chem. Rev. 46 (1977) 967.
[38] S.K. Pollack, B.C. Raine, W.J. Hehre, J. Am. Chem. Soc. 103 (1981) 6308.
[39] L.A. Hammad, P.G. Wenthold, J. Am. Chem. Soc. 122 (2000) 11203.
[40] A. Fattahi, S.R. Kass, J.F. Liebman, R.A.M. Matos, M.S. Miranda, M.F. Morais, J. Am. Chem. Soc. 125 (2005) 6116.
[41] E.P. Hunter, S.G. Lias, J. Phys. Chem. 27 (1998) 413.
[42] P.G. Wenthold, R.R. Squires, J. Am. Chem. Soc. 116 (1994) 6401.
[43] P.G. Wenthold, S.G. Wierschke, J.J. Nash, R.R. Squires, J. Am. Chem. Soc. 116 (1994) 7378.
[44] H.V. Linnert, J.M. Riveros, J. Chem. Soc. Chem. Commun. 1 (1993) 48.
[45] S.T. Graul, R.R. Squires, Mass Spectrom. Rev. 7 (1988) 263.
[46] P.J. Marinelli, J.A. Paulino, L.S. Sunderlin, P.G. Wenthold, J.C. Poutsma, R.R. Squires, Int. J. Mass Spectrom. Ion Processes 130 (1994) 89.
[47] K.M. Ervin, P.B. Armentrout, J. Chem. Phys. 83 (1985) 166.

[48] R.H. Schultz, K.C. Crellin, P.B. Armentrout, J. Am. Chem. Soc. 113 (1991) 8590.
[49] N.F. Dalleska, K. Honma, L.S. Sunderlin, P.B. Armentrout, J. Am. Chem. Soc. 116 (1994) 3519.
[50] F. Muntean, P.B. Armentrout, J. Chem. Phys. 115 (2001) 1213.
[51] M.T. Rodgers, K.M. Ervin, P.B. Armentrout, J. Chem. Phys. 106 (1997) 4499.
[52] M.T. Rodgers, P.B. Armentrout, J. Chem. Phys. 109 (1998) 1787.
[53] M.J. Frisch, G.W. Trucks, H.B. Schlegel, G.E. Scuseria, M.A. Robb, J.R. Cheeseman, J.J.A. Montgomery, T. Vreven, K.N. Kudin, J.C. Burant, J.M. Millam, S.S. Iyengar, J. Tomasi, V. Barone, B. Mennucci, M. Cossi, G. Scalmani, N. Rega, G.A. Petersson, H. Nakatsuji, M. Hada, M. Ehara, K. Toyota, R. Fukuda, J. Hasegawa, M. Ishida, T. Nakajima, Y. Honda, O. Kitao, H. Nakai, M. Klene, X. Li, J.E. Knox, H.P. Hratchian, J.B. Cross, C. Adamo, J. Jaramillo, R. Gomperts, R.E. Stratmann, O. Yazyev, A.J. Austin, R. Cammi, C. Pomelli, J.W. Ochterski, P.Y. Ayala, K. Morokuma, G.A. Voth, P. Salvador, J.J. Dannenberg, V.G. Zakrzewski, S. Dapprich, A.D. Daniels, M.C. Strain, O. Farkas, D.K. Malick, A.D. Rabuck, K. Raghavachari, J.B. Foresman, J.V. Ortiz, Q. Cui, A.G. Baboul, S. Clifford, J. Cioslowski, B.B. Stefanov, G. Liu, A. Liashenko, P. Piskorz, I. Komaromi, R.L. Martin, D.J. Fox, T. Keith, M.A. Al-Laham, C.Y. Peng, A. Nanayakkara, M. Challacombe, P.M.W. Gill, B. Johnson, W. Chen, M.W. Wong, C. Gonzalez, J.A. Pople, Gaussian 03, Revision B.05, Pittsburgh, PA, 2003.
[54] J.F.W. McOmie, D.E. West, Org. Synth., Collect. V (1973) 412.
[55] H.Y. Afeefy, J.F. Liebman, S.E. Stein, in: P.J. Linstrom, W.G. Mallard (Eds.), Neutral Thermochemical Date in NIST Chemistry Webbook, NIST Standard Reference Database Number 69, National Institute of Standards and Technology, Gaithersburg, MD 20899, June 2005 (http://webbook.nist.gov).
[56] R.G. Cooks, J.S. Patrick, T. Kotiaho, S.A. McLuckey, Mass Spectrom. Rev. 13 (1994) 287.
[57] R.G. Cooks, P.S.H. Wong, Acc. Chem. Res. 31 (1998) 379.
[58] P.B. Armentrout, J. Am. Soc. Mass Spectrom. 11 (2000) 371.
[59] J.E. Bartmess, in: P.J. Linstrom, W.G. Mallard (Eds.), Negative Ion Energetics Data in NIST Chemistry Webbook, NIST Standard Reference Database Number 69, National Institute of Standards and Technology, Gaithersburg, MD 20899, June 2005 (http://webbook.nist.gov).
[60] L.A. Hammad, P.G. Wenthold, J. Am. Chem. Soc. 123 (2001) 12311.
[61] H.A. Lardin, R.R. Squires, P.G. Wenthold, J. Mass Spectrom. 36 (2001) 607.
[62] D.J. Goebbert, P.G. Wenthold, Int. J. Mass Spectrom. 257 (2006) 1.
[63] S.J. Blanksby, G.B. Ellison, Acc. Chem. Res. 36 (2003) 255.
[64] J.E. Bartmess, in: P.J. Linstrom, W.G. Mallard (Eds.), Cluster Ions in NIST Chemistry Webbook, NIST Standard Reference Database Number 69, National Institute of Standards and Technology, Gaithersburg, MD 20899, June 2005 (http://webbook.nist.gov).